

Near-Field Electrospinning of Embedded Inorganic ZnO Nanowires

Mikkel Graugaard Antonsen

Spring semester 2014, February 3rd to August 4th



AALBORG UNIVERSITY
STUDENT REPORT

Institute of Physics and Nanotechnology

<http://www.nano.aau.dk>

Title:

Near-Field Electrospinning of Embedded Inorganic ZnO Nanowires

Subject:

Master Thesis

Project period:

Spring semester 2014, February 3rd to August 4th

Supervisors:

Esben Skovsen and Peter Fojan

Author:

Mikkel Graugaard Antonsen

Abstract:

Both NWs and nanofibers have been subject to much research in present years. A simple method to align and orientate NWs is needed for further research and commercial use.

This project intends to utilize NFES, which is a well proven method to direct-write various polymeric solution onto a conducting substrate. NFES a polymer solution with suspended NWs, would embed the NWs into the electrospun fibers.

ZnO NWs are grown with a CVD process and suspended in polymer solutions for NFES. Three transfer methods are attempted to suspend and disperse with a high yield and concentration. A NFES setup was used to direct-write the polymer solutions with embedded ZnO NWs onto sputter coated Au quartz plates and Si substrates.

The transfer rate in this work was not sufficient to yield polymer solution, with adequate concentration of dispersed ZnO NWs, to construct near field electrospun nanofibers with embedded ZnO NWs.

Print run: 4

Report page count: 27

Appendix page count: 5

Total page count: 45

Preface

This Master Thesis was written in the period February 3rd to August 4th 2014 at the Institute of Physics and Nanotechnology; Aalborg University. The thesis is based on sources from recognized scientific journals, books and web pages from universities. Figures without sources have been produced by the author with Adobe Illustrator CS6, Jmol, and MATLAB[®] 2014a.

Mikkel Graugaard Antonsen

Abbreviations

CVD	Chemical Vapor Deposition
DLSPPW	Dielectric-Loaded Surface Plasmon Polariton Waveguide
ES	ElectroSpinning
NFES	Near-Field ElectroSpinning
NW	NanoWire
OM	Optical Microscopy
PEO	Poly(Ethylene Oxide)
PVD	Physical Vapor Deposition
SEM	Scanning Electron Microscopy
VLC	Vapor-Liquid-Solid
ZnO	Zinc Oxide

Contents

Preface	i
Abbreviations	iii
Contents	v
List of Figures	vii
1 Introduction	1
1.1 Properties of ZnO Nanowires	1
1.2 Fabrication of ZnO Nanowires	3
1.3 Alignment of ZnO Nanowires	3
1.4 Electrospinning	4
1.5 Near-field Electrospinning	5
2 Materials and Methods	7
2.1 Near-Field Electrospinning	7
2.2 Fabrication of ZnO Nanowires	8
2.3 Suspension of ZnO Nanowires	9
2.4 Near-Field Electrospinning with embedded ZnO nanowires . . .	10
3 Results	11
3.1 Near-Field Electrospinning	11
3.2 ZnO Nanostructures	11
3.3 Scraped Substrate	13
3.4 Centrifuged Transfer	14
3.5 Ultrasound of Substrate	15
3.6 Sampling of Ultrasound Suspension	16
3.7 Near-Field Electrospinning with ZnO nanowires	17
4 Discussion	21
4.1 Near-Field Electrospinning	21
4.2 Growth of ZnO Nanowires	21
4.3 Transfer of ZnO nanowires	22

CONTENTS

4.4 Near-Field Electrospinning with ZnO Nanostructures	23
Bibliography	25
A List of Lab work	I

List of Figures

1.1	Histogram of the number of publications with ZnO NWs as a topic. Web of Science™ Thomson Reuters, search date July 30, 2014. . .	1
1.2	Illustration of the hexagonal wurtzite crystal structure of ZnO NWs.	2
1.3	Histogram of the number of publications with ES as a topic. Web of Science™ Thomson Reuters, search date July 30, 2014.	4
1.4	General ES setup, where a constant flow of polymer solution is subdued to a high electric field, which charges the surface and release a jet. The Jet is stretched over the travel distance which later leads to a whipping effect before the thin nanofiber reaches the collector surface in a non-woven pattern. [1, 2]	5
1.5	NFES setup; In contrast to far-field ES the needle is close to the collector surface. The needle-collector distance is typically between 500 μm and 3mm. With the shorter distance the whipping effect is avoided and the jet can be used for direct-writing on the surface. A movable collector enables direct-writing with the liquid jet. [3, 4] .	6
2.1	Schematic of the NFES setup, which was used for the fabrication of aligned nanofibers. HV-PS: High Voltage Power Supply, RS: rotations stage, PZS: xy-piezo stage, TB: Teflon Block, C: collector. [5, 6]	8
2.2	Schematic of the tube-oven setup utilized for the growth of ZnO NWs with CVD process. The source powder was placed in the center of the oven; pressure and airflow were measured and maintained with gas inlet, anemometer, pressure gauge, and valve.	9
3.1	Town-Down OM images of near-field electrospun nanofibers, with 1300 V and a needle to collector distance of 1.0 μm	12
3.2	SEM images of the second fabrication of ZnO NWs. Sample showed growth of clusters and islands of non-woven nanostructures.	13
3.3	SEM images of the third fabrication of ZnO NWs. Sample showed growth of clusters of dense packed NW structures and islands of non-woven nanostructures.	14

LIST OF FIGURES

3.4	SEM images of new and scraped surface areas of the third fabrication of ZnO NWs.	15
3.5	SEM imaging of samplings from the centrifuged transfer method of ZnO NWs.	16
3.6	SEM investigation of surface with growth of ZnO NWs before ultrasound treatment.	16
3.7	SEM investigation of surface with growth of ZnO NWs after ultrasound treatment.	17
3.8	SEM imaging of samples made from the surfactant containing the ZnO nanostructures.	18
3.9	Top-down OM images of the investigation of electrospun nanofibers with transferred ZnO NWs from ultrasound.	18
3.10	SEM investigation of electrospun nanofibers with transferred ZnO NWs from ultrasound.	19
3.11	SEM investigation of electrospun nanofibers with transferred ZnO NWs from ultrasound after the burning process.	20

Introduction

The demand to reduce dimensions and enhance the efficiency electronic devices is a continuous goal and more research is conducted on the nanoscale. The research of ZnO nanowires have increased since the start of 2000, see Figure 1.1, though the rate of yearly publications has decreased due to new found interest in the one dimensional carbon nanotubes and two dimensional nanostructure graphene [7]. Still the applications of ZnO NWs is an area of interest, as they can be used as ultra violet light emitters, gas sensors, piezoelectric devices, transparent electronics, photosensors, and in optoelectronics. [8, 9, 10]

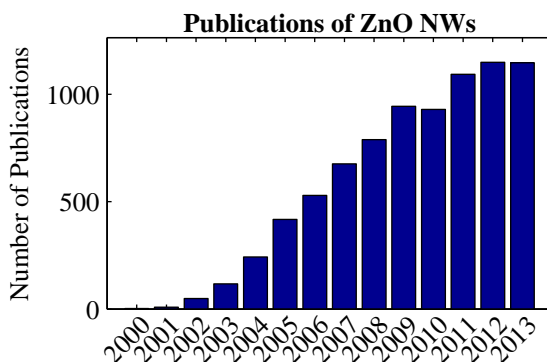


Figure 1.1: Histogram of the number of publications with ZnO NWs as a topic. Web of ScienceTM Thomson Reuters, search date July 30, 2014.

1.1 Properties of ZnO Nanowires

ZnO nanowires are inorganic II-VI semiconductors of one dimensional nanostructure, with a wurtzite crystal structure. Each Zn atom is hexagonal closest-packed bound to four oxygen atoms as a tetrahedral structure and vice versa,

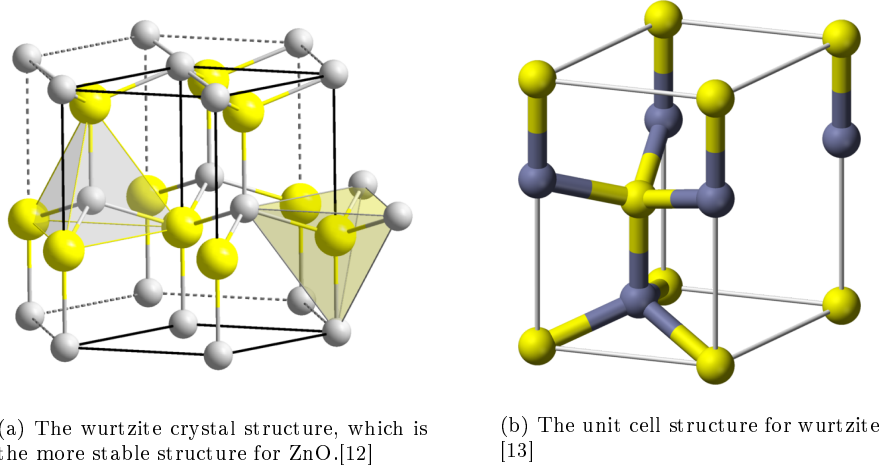


Figure 1.2: Illustration of the hexagonal wurtzite crystal structure of ZnO NWs.

see Figure 1.2. Other crystal structures for ZnO is zinc blende and rocksalt, while wurtzite is the more stable structure at 300 K. [11]

The interest of ZnO NWs have increased as ZnO shows great potential low cost and commercial application in optoelectronics. The physical properties of ZnO is a high band gap of 3.37 eV at 25 °C and a exciton binding energy of 60 meV, which is considerably higher than those of GaN and ZnSe - 25 meV and 26 meV respectively [11]. Table 1.1 lists the physical properties of ZnO. [7, 11, 10]

Physical properties	
Lattice constants	$a = 0.32469 \text{ nm}, c = 0.52069 \text{ nm}$
Density	5.606 g/cm^3
Band gap	3.37 eV
Exciton binding energy	60 meV

Table 1.1: Physical properties of ZnO [11, 9].

One of the interesting applications of ZnO NWs is as dielectric loaded surface plasmon polariton waveguides (DLSPPWs). Surface plasmons are surface bound electromagnetic modes, which propagates along metal-dielectric interfaces, as the the intensity normal to the propagation is exponentially decaying. These surface plasmons have shown great promise in the world of nanoscale optoelectronics, which can reduce the dimensions of photonic integrated circuits. [5]

1.2 Fabrication of ZnO Nanowires

Several growth protocols are available for synthesizing high quality ZnO nanowires, which have individual advantages and disadvantages. The methods described are vapor-liquid-solid, physical vapor deposition, chemical vapor deposition, metal-organic chemical vapor deposition and hydrothermal-based chemical approach. [7]

The Vapor-Liquid-Solid (VLC) method was first described by Wagner and Ellis in 1964, where they grew crystalline whiskers of Si from vapor sources of Si with gold particles as catalyst for growth. A vapor phase of high purity ZnO led by an inert gas crystallizes under a metal catalyst, and growth of nanostructures is initiated. The diameter of the grown nanostructures can be controlled by the size of the metal catalyst. To grow ZnO nanowires with the VLC method a porous Si wafer with sputter-coated Au particles is placed in a tube furnace. The nanowires are grown at temperatures above 600 °C with a pressure ranging from 3 to 30 Torr under a constant flow rate of 100 to 250 *SCCM* argon. [7]

Another method is the physical vapor deposition (PVD), similar to the VLC, a source of ZnO is vaporized at high temperatures and transported with a gas flow to a deposition area at a lower temperature. The PVD technique is further specified with electron beam PVD, arc physical PVD, pulse laser deposition and ion beam sputtering. Growth of ZnO nanowires is usually achieved with a 1:1 source of ZnO and C heated in a tube furnace. The vaporized ZnO:C is transported with a constant flow of Ar or O to a Si or sapphire substrate, where the ZnO crystallizes at temperatures ranging from 150 to 550 °C. [7]

The chemical vapor deposition (CVD) is similar to the previous methods, the source is diffused to the substrate and adsorbed onto the surface of the substrate. A chemical reaction will deposit the solid, the by-products will desorb from the surface and diffuse into the gas-stream. The parameters are similar to those of the PVD and the by-products can be corrosive depending on the reactions at the deposition. [7]

Aqueous synthesis of ZnO nanowires can be alternative method for fabrication. Lin et al. have demonstrated a bottom-up approach for synthesizing aligned ZnO nanowires from an aqueous solution of zinc nitrate and hexamethylenetetramine, via local heating and directed electric field alignment. [14]

[11, 7, 15]

1.3 Alignment of ZnO Nanowires

As the nanoscale development has increased, so has the need to align nanostructures, especially NWs and nanotubes, with high accuracy and efficiency. So they may properly located, orientated and spaced. Several methods have been utilized for this purpose, some examples are a dielectrophoresis method [16], blown bubble technique [17], Langmuir-Blodgett technique [18], and ion beams to align and bend ZnO NWs after growth. [16, 17, 18, 19]

Another way of aligning NWs and nanotubes is to suspend them in a polymer solution, which can be used for electrospinning (ES). Figure 1.3 shows a histogram of publications for each year with ES as topic. The high interest for the low-cost fabrication of 1 dimensional structures facilitates numerous research areas. By decreasing the fiber diameter below a critical value increases the Young's modulus compared to the bulk structure. [20] Chang et al. [21] demonstrated piezoelectric properties of direct written electrospun nanofibers.

It is of high interest to utilize the advantage of suspending NWs and nanotubes in a organic polymer solution, which can be converted into well aligned and uniform nanofibers with NWs and nanotubes embedded. The organic fibers can following be removed, with a burning process leaving only the embedded inorganic materials.

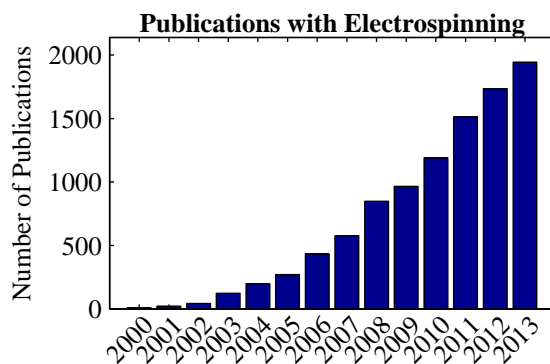


Figure 1.3: Histogram of the number of publications with ES as a topic. Web of Science™ Thomson Reuters, search date July 30, 2014.

1.4 Electrospinning

ES is a proven method for producing continuous micro- and nanoscale fibers, from a polymeric solution with a high DC electric field. A wide variety of synthetic and natural occurring polymer solution can be electrospun with appropriate parameters. [4]

The process uses a high electric field, polarizing a polymer droplet and induce electrostatic repulsion at the surface. The electrostatic repulsion increases with increasing applied voltage, which drags the droplet towards a grounded conducting collector, elongating the hemispherical surface into conical shape, known as a Taylor cone. Surfactants can be mixed with the polymer in order to reduce the surface tension. From the Taylor cone a jet is dragged by the electric field towards the grounded collector, while is stretches and evaporates into a solid string. A constant flow of polymer must be fed in order to maintain

a constant volume for the droplet. After a certain travel distance the electrostatic repulsion and solidification changes the uniaxial travel from the origin into a randomized motion, described as bending instabilities and a whipping effect. This causes a serious increase in travel distance thinning the width of the fiber into micro- or nanoscale. When the fiber arrives at the collector surface it is deposited as a non-woven structure. The general setup for ES is sketched in Figure 1.4. [1, 2, 4]

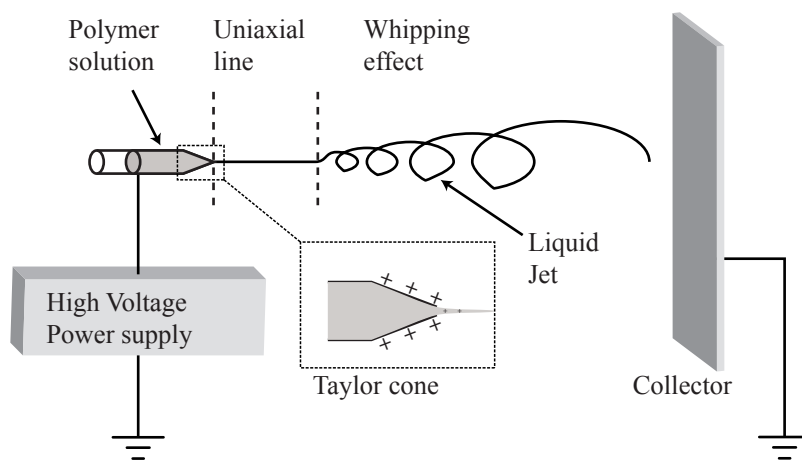


Figure 1.4: General ES setup, where a constant flow of polymer solution is subdued to a high electric field, which charges the surface and release a jet. The Jet is stretched over the travel distance which later leads to a whipping effect before the thin nanofiber reaches the collector surface in a non-woven pattern. [1, 2]

Several alternate ES setups have been investigated, for instance coaxial ES combines two polymers into one fiber. Other methods focus on yield increase of fibers; needle-less ES, Rotating drum and translating spinneret ES, rotating electrodes ES. Also ES with focus on orientation of fibers are of interest, among these setups are rotating disk ES, non-bending instability ES, and near-field ES (NFES). [1, 2, 4]

1.5 Near-field Electrospinning

Continuous NFES is an alternate setup from the general ES, where the needle to collector distance is greatly reduced to avoid the bending instabilities of the jet, making it suited for direct-writing. The method was reported by Sun et al. [3], where a NFES setup was constructed to continuously develop and deposit solid nanofibers in an aligned pattern. The needle to collector distance is typically

1. INTRODUCTION

in the range of $500\ \mu\text{m}$ and $3\ \text{mm}$, Figure 1.5 illustrates the NFES setup. With NFES the volume of deposited fibers are small, and a single droplet of polymer is sufficient for direct-writing, neglecting the need of a constant flow of polymer. The collector is often mounted on a xy-piezo stage for precise control of the fiber deposition and orientation. The voltage for continuous ES is decreased with the decreased distance, and the electric field alone is often not sufficient to overcome the surface tension of the polymer droplet. Chang et al. [22] described a method to initiate the jet flow, by mechanically probing the droplet and drag a thin fiber from the surface to the collector surface. Furthermore, Bisht et al. [23] have reported continuous NFES with a superelastic polymer ink, with voltages down to 200 V.

[2, 3, 4]

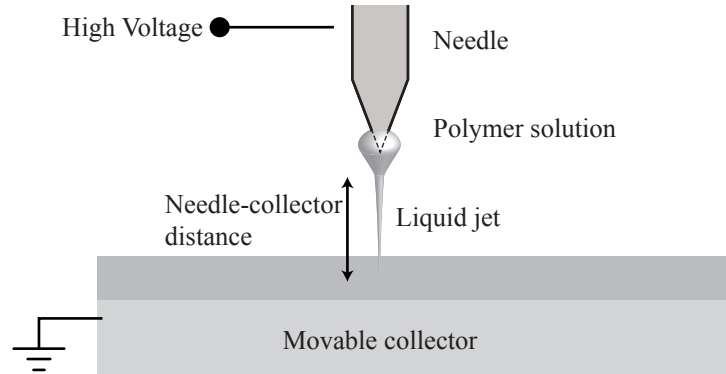


Figure 1.5: NFES setup; In contrast to far-field ES the needle is close to the collector surface. The needle-collector distance is typically between $500\ \mu\text{m}$ and $3\ \text{mm}$. With the shorter distance the whipping effect is avoided and the jet can be used for direct-writing on the surface. A movable collector enables direct-writing with the liquid jet. [3, 4]

NFES have been used as a method to fabricate and deposit DLSPPWs of polymer nanofibers on Au coated substrate. [5] Successful electrospinning of CdS NWs embedded into a polymer was reported by Bashouti et al. [24]. The CdS NWs was purified and dispersed in a 10 % w/w solution. Another method of aligning NWs is to grow them within electrospun nanofibers as reported by Rinaldi et al. [25]. The group grew TiO_2 NWs of several mm within near field electrospun fibers. Dong et al. [26] were able to fabricate $\text{Y}_2\text{O}_3:\text{Eu}^{3+}$ nanofibers with an electrospinning setup.

Materials and Methods

Table 2.1 list the materials used for laboratory work.

Material	Manufacturer	CAS number	Note
tert-Butanol	Sigma-Aldrich	33067 ALDRICH	Purity $\geq 99.5\%$
Poly(ethylene oxide)	Sigma-Aldrich	189456 ALDRICH	$M_v \sim 900,000\text{g/mol}$

Table 2.1: Table of materials used in laboratory work.

2.1 Near-Field Electrospinning

The setup for the NFES is a homemade setup at the institute, see Figure 2.1. A syringe is mounted on a block, which is adjusted in three directions. The collector is fixed on a xy-piezo stage with a Teflon block between to separate the electronics. A rotation stage enables mounting of new collectors, without lifting the syringe. A 3000 V power supply supplied the voltage difference between needle and collector. NFES was started by lowering the syringe needle to the near-field range of the collector, and a droplet of polymer solution added to the needle tip. The electric field was applied and the jet from the Taylor cone initiated by tapping a tungsten tip to the droplet surface, described by Chang et al. [22]. The xy-piezo stage moved the collector at a speed of 200 mm/s in parallel lines with a 110 μm distance.

The collector material were both Au sputter coated rectangular quartz plates and rectangular pieces of Si wafer.

Preparation of Polymer Solution

Earlier work during previous semester have investigated the influence of various parameters for polymer solutions to to continuous NFES. Both tert-butanol and ethanol were used to lower the surface tension of the solution, Table 2.2 lists the PEO solution made for the NFES fabrication of nanofibers. The PEO powder

2. MATERIALS AND METHODS

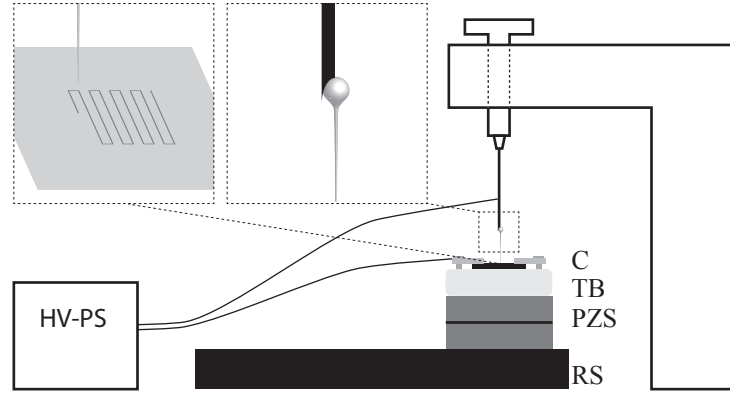


Figure 2.1: Schematic of the NFES setup, which was used for the fabrication of aligned nanofibers. HV-PS: High Voltage Power Supply, RS: rotations stage, PZS: xy-piezo stage, TB: Teflon Block, C: collector. [5, 6]

was mixed with the alcohol and diluted to the final volume. The solution was dissolved by stirring the mixture at 200 rpm on a 50 °C plate for 24 hours.

#	PEO [%]	Ethanol [%]	tert-Butanol [%]	Ratio
1	4	10	0	0.116
2	4	5	0	0.055
3	4	0	24	0.333

Table 2.2: Specifications for the polymer solutions, used for the NFES. Ratios are calculated as the alcohol/water mass ratio.

2.2 Fabrication of ZnO Nanowires

The ZnO nanowires were produced in a tube furnace; Nabertherm model R40/500/12-B170 with a Buch & Holm controller.

Pure ZnO and C powder were mixed 1:1 *mol*, loaded into a quartz basin and dried for one hour at 110 °C. The dried product was placed in the center of the tube furnace, and a degreased Si wafer piece placed at the outer edge of the furnace. The inner tube was pumped down to 0.1 *mbar*, after which a constant airflow of 5.2 *SCCM* dried air was supplied increasing the pressure to 2 *mbar*. The pressure was further increased to 4 *mbar* and maintained with a valve at the pump. The temperature was raised to 1050 °C and maintained for 1.5 *h*. During temperature increase the tube pressure and airflow were regulated to the mentioned parameters. The setup for the CVD process is sketched in Figure 2.2.

After cooling the tube was slowly vented and opened. The samples were gently removed and first microscopic investigation showed growth upon the Si

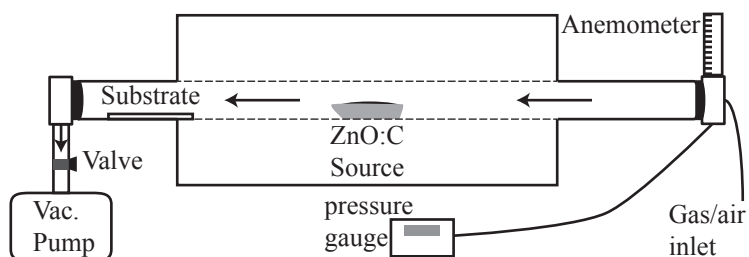


Figure 2.2: Schematic of the tube-oven setup utilized for the growth of ZnO NWs with CVD process. The source powder was placed in the center of the oven; pressure and airflow were measured and maintained with gas inlet, anemometer, pressure gauge, and valve.

substrate surface. The samples were further analyzed and investigated with optical microscopy (OM) and scanning electron microscopy (SEM).

2.3 Suspension of ZnO Nanowires

Three types of investigations were done for sufficient yield transfer of the grown ZnO NWs to a polymer solution. To verify a successful transfer of ZnO NWs to a polymer solution, samplings was made and investigated with OM and SEM. The samples was heated to $400\text{ }^{\circ}\text{C}$ for 25 min to remove organic compounds.

Scraping

The substrates surface area of confirmed growth was scraped with a sharp razor blade and the powder mixed with PEO powder and later alcohol following #3 in Table 2.2. The mixture was then diluted to the final volume and stirred at 200 rpm on a $50\text{ }^{\circ}\text{C}$ plate for 24 hours. The solution was exposed to a short treatment of ultrasound before electrospinning, to ensure an evenly dispersion of the ZnO NWs.

Centrifuge

The ZnO NWs were scraped from the Si surface and transferred to a prepared polymer solution, following #3 in Table 2.2. To disperse the NWs the solution was centrifuged and samplings were made onto Si wafer pieces, to investigate the dispersion with SEM.

Ultrasound suspension

A substrate with confirmed growth of ZnO nanostructures, was placed in a ultrasonic bath with ethanol and exposed to a low energy ultrasound treatment. The substrate was gently removed from the solution and investigated with

SEM. The solution was mixed with PEO powder and diluted to a final volume following #1 in Table 2.2, and dissolved with stirring and heating.

2.4 Near-Field Electrospinning with embedded ZnO nanowires

The solutions were prepared as described in previous section. The needle was positioned 1.0 mm from the collector surface and a droplet of polymer solution was added to the tip. The high voltage was applied to the setup and the program for stage movement initiated. A voltage of 1450 V for the NFES was chosen, as this yielded the most aligned and uniform fibers. Often following runs were conducted, as the jet stream was stable. Further analysis of the fabricated nanofibers was conducted with OM and SEM. To remove the electrospun polymer nanofibers the samples was burned in an $400\text{ }^{\circ}\text{C}$ oven for 25 min.

Results

3.1 Near-Field Electrospinning

The NFES setup was successfully used to fabricate aligned nanofibers from a variety of polymeric solution. The electric field alone was not sufficient to initiate a jet from the Taylor cone formed by the droplet. Tapping the droplet with a wolfram needle started a continuous jet, which was applicable for direct-writing on the collector surface. Au coated quartz pieces as collector material was well suited for NFES and yielded high rate of well aligned nanofibers.

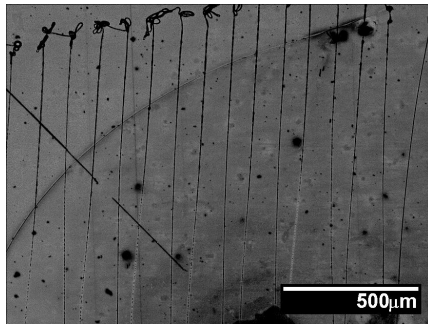
The obtained images from the top-down OM, have been cut and converted to greyscale with MATLAB, in the lower right corner a length scale have been added. Figure 3.1a shows an overview of the pattern investigated with a top-down optical microscope. Often multiple jets was continuously flowing from the droplet, which caused overlapping patterns. The well-aligned pattern is presented in Figure 3.1b. The nanofibers have a uniform structure with small beads, and a $100 \mu m$ spacing. The width of the fibers ranged from 1 to $4 \mu m$ with formation of beads, a zoom of a single fiber is shown in Figure3.1c.

3.2 ZnO Nanostructures

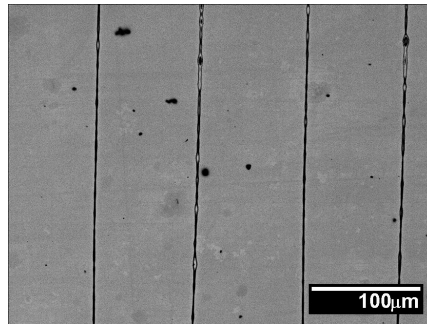
Several successful productions of ZnO NWs were conducted with the CVD process described in Section 2.2. The bottom-up approach had a low yield as much of the source were adsorbed elsewhere in the tube-oven. The growth was visible as a white area on the Si wafer, when the substrate was removed from the tube-oven.

The samples were analyzed with SEM and showed a wide variety of nanostructures, including nanobelts, nanoblades, nanoneedles, and NWs. A scale length is shown in en lower right corner of the SEM images, which is added with a ImageJ v. 1.48. Overview of the second fabrication is shown in Figure 3.2a. The surface is covered with clusters of non-woven nanostructures, with little or no indication of structures resembling NWs. The structure of the clusters were nonuniform and their size decreased from the center of growth to the edges. A typical cluster located at the edge of growth is shown in Figure 3.2b. Nearer the center of growth the size of clusters and the non-woven structures

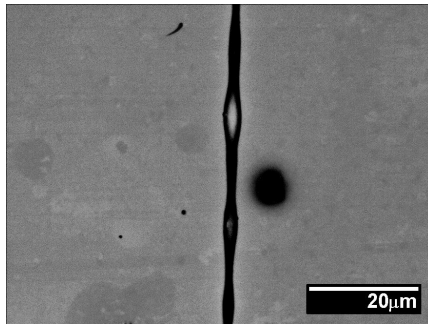
3. RESULTS



(a) Overview image showing the pattern of the near-field electrospun nanofibers.



(b) Zoom of the surface illustrating the uniform aligned nanofibers separated by $100\ \mu\text{m}$ written on the collector surface.



(c) Zoom of a single nanofiber, with a width ranging from 1.5 to $3.5\ \mu\text{m}$ due to beads formation.

Figure 3.1: Town-Down OM images of near-field electrospun nanofibers, with $1300\ \text{V}$ and a needle to collector distance of $1.0\ \mu\text{m}$.

increased as shown in Figure 3.2c. Zoom of the structure located at the center showed growth of a ZnO structure with no resemblance to NWs, see Figure 3.2d.

Following fabrications had a higher yield of structures similar to ZnO NWs. These structures were located at the outer edges of growth, See Figure 3.3a. The center of growth had a higher rate of structures, resembling the structures from the previous discussed fabrication. The size of the NW clusters increased within a short length, before non-woven structures became dominant on the surface. The growth area of NWs typically spanned a length $8\ \text{mm}$ from the edge towards the center of growth. A single cluster consisting of NW structures is shown in Figure 3.3b. The cluster is $10\ \mu\text{m}$ in length and $6.5\ \mu\text{m}$ in width. Further analysis clearly show long hexagonal ZnO NWs along with nanoblades, see Figure 3.3c and 3.3d.

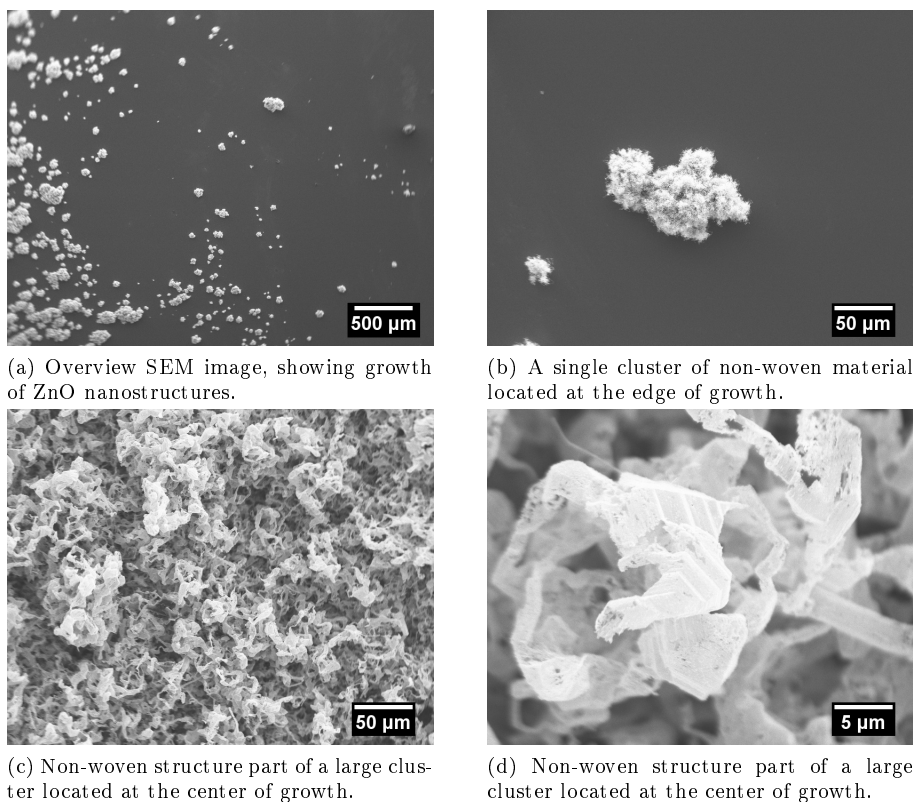
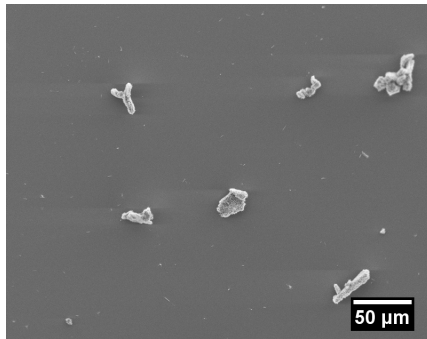


Figure 3.2: SEM images of the second fabrication of ZnO NWs. Sample showed growth of clusters and islands of non-woven nanostructures.

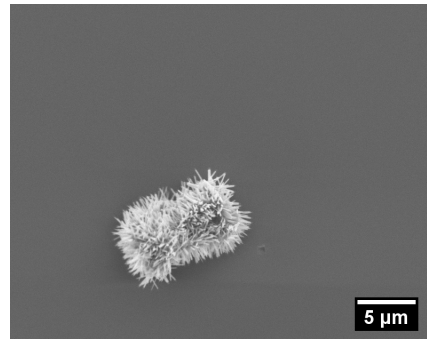
3.3 Scraped Substrate

The substrates of confirmed growth were analyzed with SEM before and after the surfaces were scraped. Figure 3.4a and 3.4b show the surface of the third fabrication of ZnO NWs. Several clusters of NWs are present in the scanned areas. After the substrate was scraped the same area of growth was investigated, which is shown in Figure 3.4c and 3.4d. Scratches are cut into the substrate from the razor blade and the clusters of NWs are removed. After the powder was suspended in the polymer solution following the procedure in Section 2.3, samplings was made to analyze the suspension and dispersion of the NWs in the solution. No NW structures were observed and following NFES of the solution yielded well-aligned nanofibers, as described in Section 3.1, with no indication of embedded NWs.

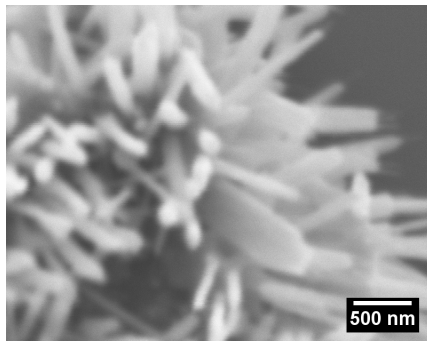
3. RESULTS



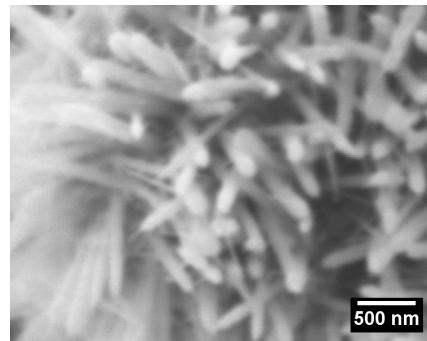
(a) Overview of the surface of growth, with several clusters of dense packed nanostructures are present.



(b) Zoom of a single cluster of $10\ \mu\text{m}$ in length and $6.5\ \mu\text{m}$ in width with high density of ZnO nanostructures.



(c) Further zoom of the cluster, several hexagonal nanostructures with a width of approximately $150\ \text{nm}$ and blade structures are visible.



(d) Second zoom a cluster, with several hexagonal nanostructures with a width of approximately $150\ \text{nm}$ and blade structures.

Figure 3.3: SEM images of the third fabrication of ZnO NWs. Sample showed growth of clusters of dense packed NW structures and islands of non-woven nanostructures.

3.4 Centrifuged Transfer

The substrate surface areas of confirmed were scraped and investigated as previous samples. The powder was scraped directly from the substrate surface in a prepared polymer solution. After the solution was centrifuged samplings was made to analyze suspension and dispersion of ZnO nanostructures. Investigation showed multiple structures within the sampling area, which is shown in Figure 3.5a. The clusters are widely spread within the sampling area, however no structures showed similarity to NWs. A further zoom of a single cluster is shown in Figure 3.5b. The structures did not contain NWs.

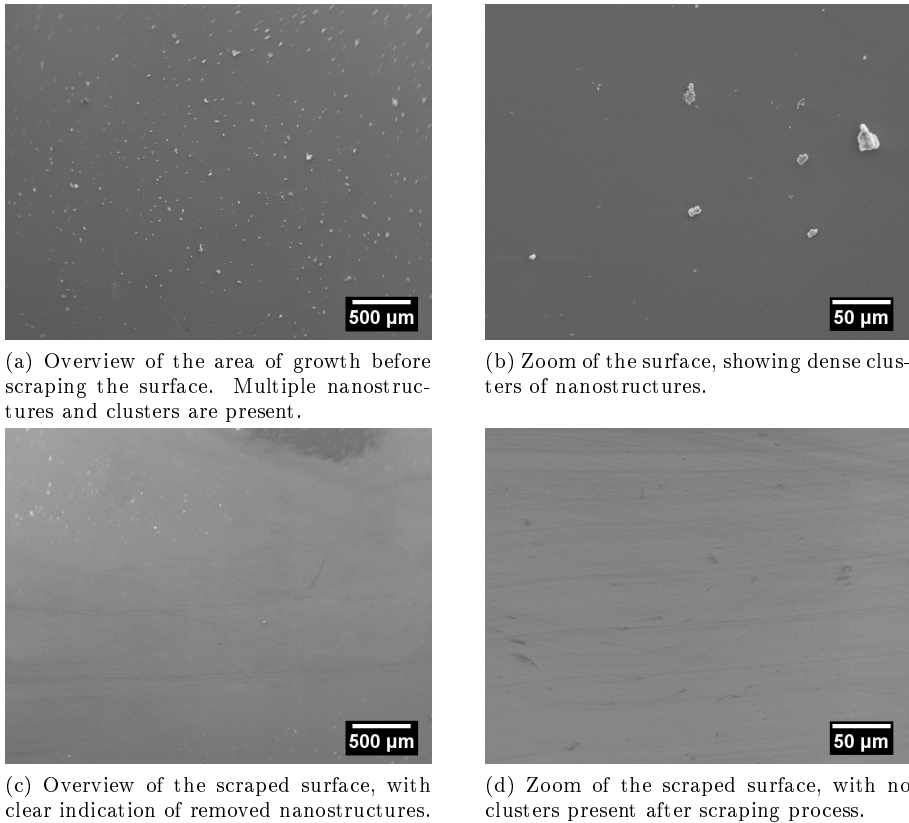


Figure 3.4: SEM images of new and scraped surface areas of the third fabrication of ZnO NWs.

3.5 Ultrasound of Substrate

To analyze the effect of using ultrasound to release the nanostructures from a substrate into ethanol, the substrates were analyzed with SEM. Figure 3.6a show the surface area of growth. The surface is covered by a variety of ZnO nanostructures, where the NW and nanoneedle structures were located at the outer edge of the growth area. The NW structures were gathered as clusters, as shown in Figure 3.6b.

After the ultrasound burst the majority of the clusters and nanostructures covering the surface were removed from the surface previously analyzed, which is shown in Figure 3.7a. Many of the clusters consisting of nanobelts were removed or dismantled, see Figure 3.7b. Further investigating closer to the center of growth revealed multiple trails from previously located clusters containing NWs, as shown in Figure 3.7c. The NW cluster were nearly completely removed from the surface by the ultrasound burst, leaving only faint marks

3. RESULTS

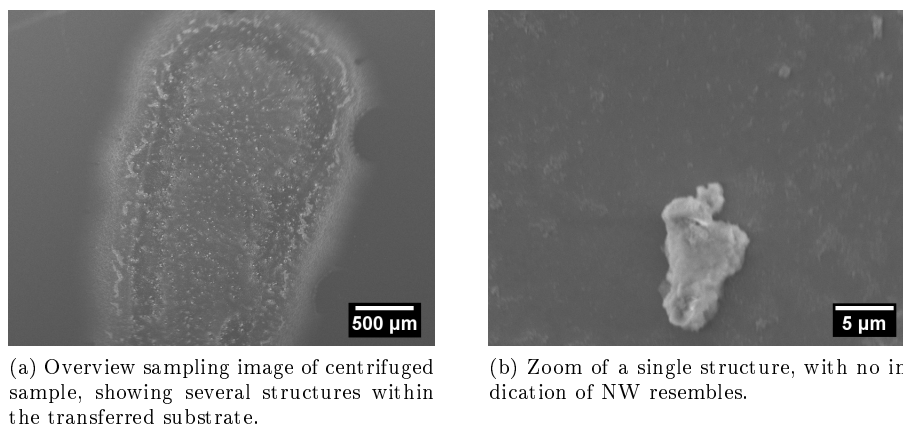


Figure 3.5: SEM imaging of samplings from the centrifuged transfer method of ZnO NWs.

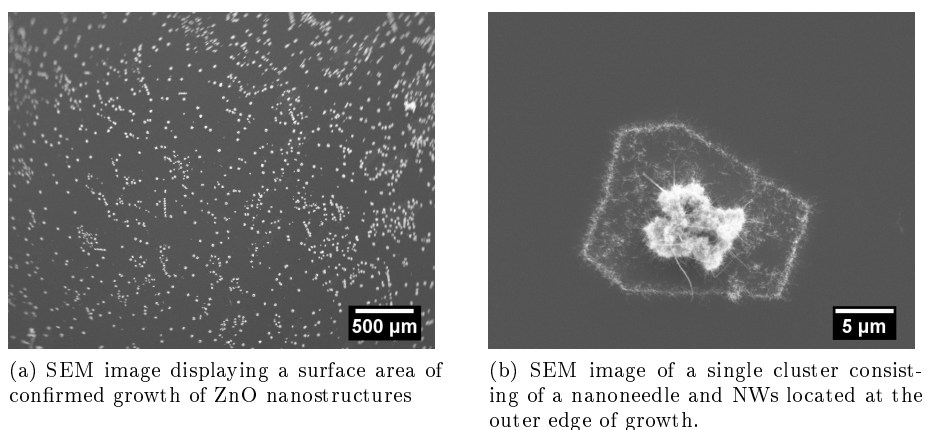


Figure 3.6: SEM investigation of surface with growth of ZnO NWs before ultrasound treatment.

from the growth area. Figure 3.7d displays the frequently observed indications of removed a NW cluster.

3.6 Sampling of Ultrasound Suspension

The surfactant containing the ZnO nanostructures were sampled to investigate the dispersion of structures. The concentration was low, and only few of the structures resembled NWs. Figure 3.8a display the few structures found in the sampling of the surfactant. Further analyzing showed fragmented structures from nanobelt clusters and only few with similarity to NWs, see Figure 3.8b.

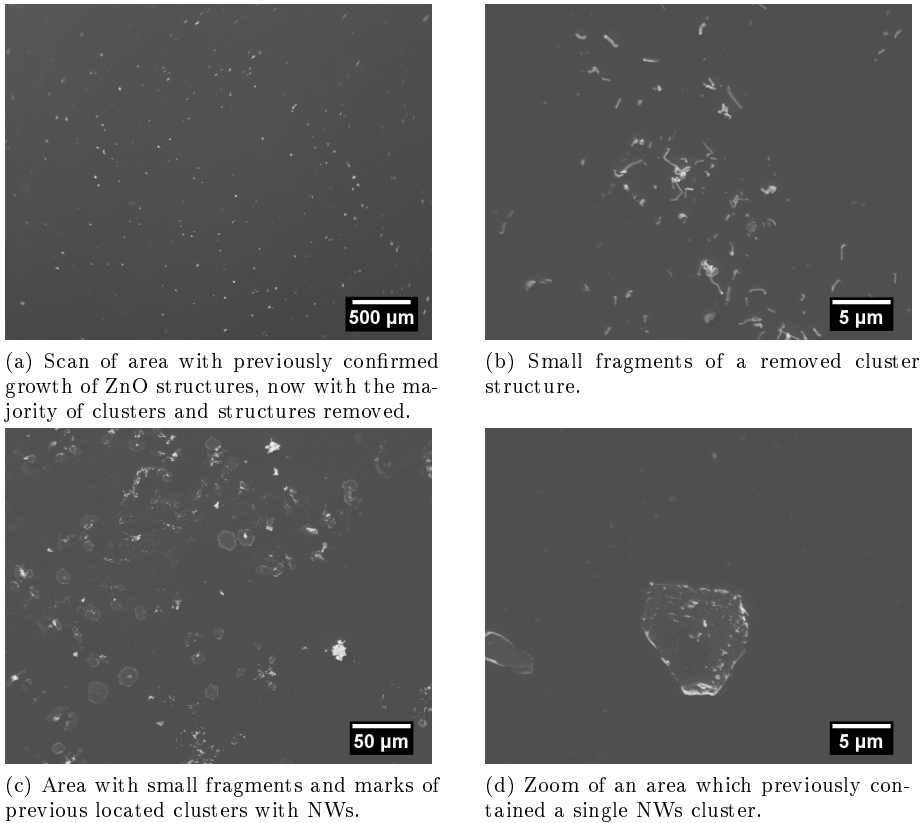


Figure 3.7: SEM investigation of surface with growth of ZnO NWs after ultrasound treatment.

3.7 Near-Field Electrospinning with ZnO nanowires

The near-field electrospun nanofibers were analyzed with both OM and SEM. Si wafer pieces were chosen as collector material to ensure proper conductance for SEM imaging.

Top-down Optical Microscopy

The electrospun fibers were well aligned in the ordered pattern, with a high probability for multiple jet streams flowing simultaneously, leading to overlapping patterns. Figure 3.9a displays an overview image of the electrospun fibers. The alignment and spacing were similar to previous NFES investigations. The fiber thickness ranged from 0.4 to 0.8 μm , and showed a solid surface. Zoom of the electrospun fibers is shown in Figure 3.9b. After a burning process of the sample, all fibers removed almost completely, and no NW structures were visible on the surface.

3. RESULTS

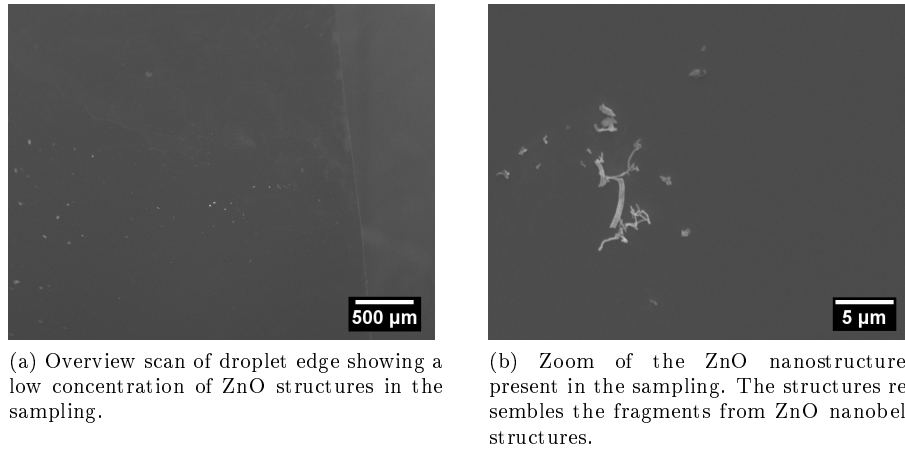


Figure 3.8: SEM imaging of samples made from the surfactant containing the ZnO nanostructures.

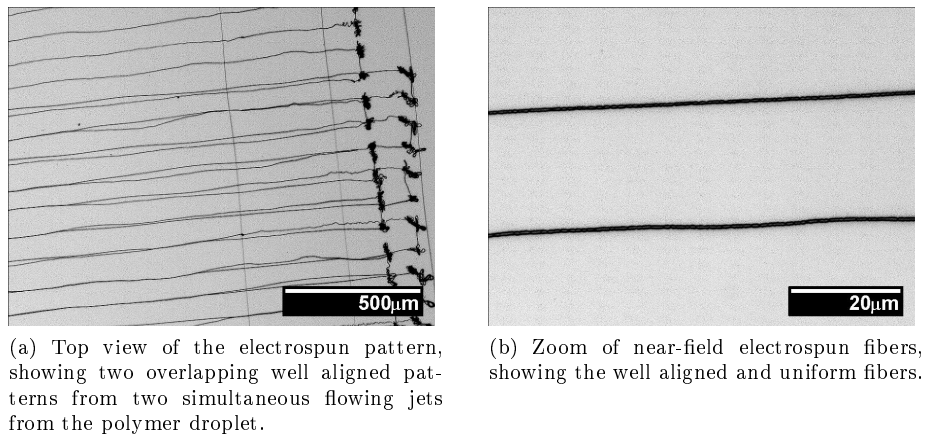
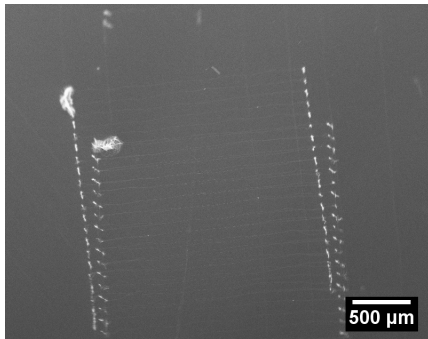


Figure 3.9: Top-down OM images of the investigation of electrospun nanofibers with transferred ZnO NWs from ultrasound.

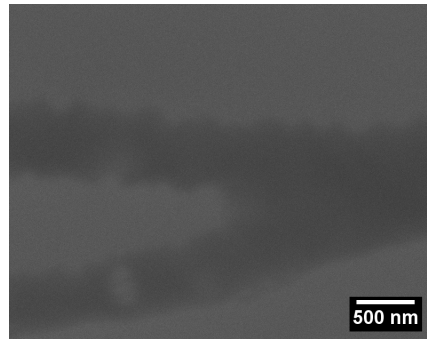
Scanning Electron Microscopy

An overview SEM image of the electrospun fibers in Figure 3.10a. The pattern is identical to the investigations conducted with OM. Further investigation showed no sign of embedded ZnO NWs or structures. Larger compounds of electrospun fibers were present at edge corner of the ES pattern, see Figure 3.10c.

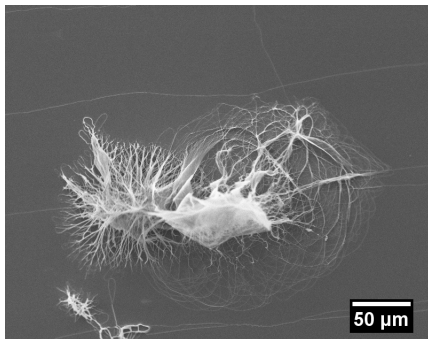
After the burning process only a faint trail was left upon the surface visible with SEM, see Figure 3.11a. No structures with dimensions of NWs were observed on the surface of the burned sample. The only structures were mi-



(a) Overview of the electrospun nanofibers. Two patterns are present in the investigated area, as two jets were flowing from the polymer droplet.



(b) Zoom of the electrospun fibers

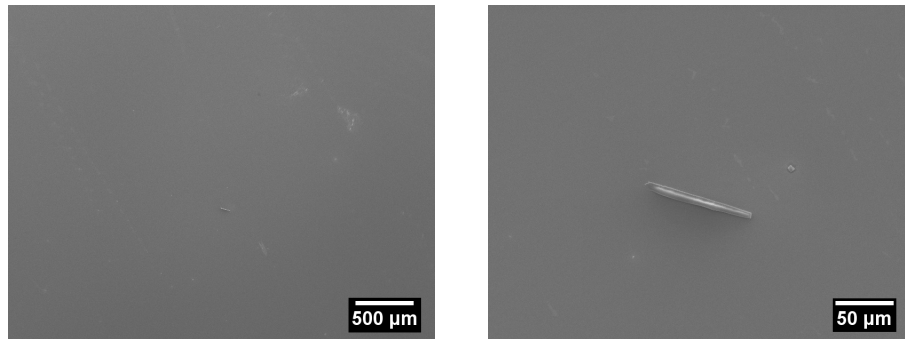


(c) Larger compound of electrospun fiber, which is deposited in a non-ordered structure.

Figure 3.10: SEM investigation of electrospun nanofibers with transferred ZnO NWs from ultrasound.

crosscale structures were located within the area of the electrospun pattern, see Figure 3.11b.

3. RESULTS



(a) Overview of the electrospun nanofibers after the burning process. Only a faint trail is left of the electrospun pattern.

(b) Zoom of a single structure located within the electrospun pattern with a length of approximately $100\ \mu\text{m}$ and width of $7\ \mu\text{m}$.

Figure 3.11: SEM investigation of electrospun nanofibers with transferred ZnO NWs from ultrasound after the burning process.

Discussion

4.1 Near-Field Electrospinning

With the NFES setup several, polymer solutions and working parameters have been investigated, in order to fabricate continuous orientated and uniform nanofibers. During previous semester, the impact of surfactant ratio and concentration of polymer where examined. The most uniform fibers where obtained with a polymer solution of 3 % PEO dissolved in en ethanol/water 0.054 mass ratio. A 500 μm needle to collector distance and electric field of 1.4 MV/m yielded the highest success rate for continuous NFES, with the mentioned PEO solution. During this work, the needle to collector distance was increased to 1000 μm in order to obtain a higher probability for the embedded NWs to flow and align within the electrospun fibers. To avoid electro spraying the polymer concentration was increased from 3 % to 4 %. The fibers fabricated were well orientated and uniform, with a width of 0.4 to 0.8 μm .

4.2 Growth of ZnO Nanowires

With the CVD process several fabrications of ZnO nanostructures were conducted. The parameters of growth were a 1:1 C:ZnO ratio, a maintained tube pressure of 4 *mbar*, airflow of 5.2 *SCCM*, baking temperature of 1050 °C maintained for 1.5 *h*. Initial fabrications were of lowest quality, compared to the following productions, which contained a larger number of NWs in the growth area. Multiple ZnO nanostructures were observed with SEM, including nanobelts, nanoblades, nanoneedles and nanowires, confirming the vast morphology of ZnO structures. The desired NW structures were located at the outer edges of growth area, often assembled with similar structures, as nanoneedles and nanoblades in larger clusters. Towards the center of growth the clusters dimensions grew and nanobelt structures dominated the surface. Investigations of the clusters of nanobelts located single NW and nanoblade structures entangled within the larger nanobelt structures, which would indicate that NW structures exist within the larger clusters.

4.3 Transfer of ZnO nanowires

The three methods for transferring all removed ZnO NWs and clusters, from the surface of the substrates, with confirmed growth.

Scraped Transfer

The first and second method both scraped the surface, and transferred the scraped power to a polymer solution. The polymer solutions for these methods used tert-butanol as a surfactant; as the rate of evaporation is lower than ethanol.

For the first method, the powder scraped lose from the substrates was first mixed with PEO powder to disperse the NWs throughout the solution. Adding alcohol and diluting with water after mixing the powders, was considered the procedure with most optimal condition of evenly dispersion. The solutions were exposed to a short low energy ultrasound burst; too further disperse the single NWs through the solution. The yield of ZnO NWs suspended was very low, with only few structures within a large sampling volume. The fibers produced by NFES the polymer were identical to earlier produced fibers, with no indication of embedded ZnO NWs or similar structures. The transfer yield is too low with the method, or the NWs precipitates, rearrange into larger clusters, or broken at some point during the suspension or dispersion.

Centrifuged Transfer

With the second method a larger area of the surface with growth were scraped, thus including the larger cluster of nanobelts. The powder was transferred to a prepared solution, and centrifuged in order to precipitate the larger clusters and suspend smaller structures of nanoneedles, nanoblades and NWs. It was estimated that single pieces and entangled pieces of NWs and similar structures would disperse, as the clusters diffused through the solution. Samplings of the solutions contained several structures, although none of the desired NWs. As for the first method, the electrospun fibers produced of the polymer were identical to the others previously described.

Ultrasound Transfer

The third method released the ZnO nanostructures from the substrate, with an ultrasonic burst. Whole substrates with growth on the surface where immersed in ethanol, thus including an even more vast morphology of ZnO nanostructures than the two previous transfer methods. SEM investigations of the treated surfaces, showed that several of the earlier confirmed grown ZnO structures, were removed and suspended into the ethanol solution. Fragments of the nanobelt clusters were still present on the surface, some having similar dimensions as NWs, but no hexagonal structure. The method was clearly more efficient to transfer the grown ZnO nanostructures from the surface. However, the method

required a significantly larger volume of alcohol, than the two previous methods, to immerse the substrate completely. Hence, the surfactant solution had a low concentration of suspended ZnO NWs. After the PEO was completely dissolved in the solution, samplings showed identical results as the two other methods. Multiple nanostructures were present, while no NWs were located amongst them. The structures are considered to be pieces of PEO, which have not been completely dissolved.

The NFES of the polymer solution fabricated continuous orientated thin uniform nanofibers. OM and SEM analysis was unable to observe any abnormality of the fibers that could indicate NW structures embedded within them. After a burning process the organic fibers were nearly completely removed from the substrates, leaving only a faint trail on the surface. Further SEM investigation confirmed that no NWs had been embedded within the fabricated patterns. The only observed structures were large rectangular pieces, which had no specific orientation or alignment towards the electrospun pattern. The rectangular pieces had some nanoblade resemblance in dimensions, but were not considered relevant for the NFES.

4.4 Near-Field Electrospinning with ZnO Nanostructures

NFES is a simple method to fabricate and orientate polymeric nanofibers on a conducting collector. The nanofibers fabricated during this work, were successfully electrospun from various polymer solution. Although the intended purpose to embed ZnO NWs into the nanofibers was not. The concentration and purity of the fabricated ZnO NWs are deemed to low to proper NFES purposes. Even though several similar structures were present on the fabricated substrates.

Bibliography

- [1] D. Li and Y. Xia. Electrospinning of nanofibers reinventing the wheel? *Advanced Materials*, 16(14):1151–1170, JUL 2004. doi:10.1002/adma.200400719.
- [2] Zhenyu Li and Ce Wang. *One-Dimensional nanostructures: Electrospinning Technique and Unique Nanofibers*. Springer Berlin Heidelberg, 2013.
- [3] D. H. Sun, C. Chang, S. Li, and L. W. Lin. Near-field electrospinning. *Nano Letters*, 6(4):839–842, APR 2006. doi:10.1021/nl10602701.
- [4] W. S. Khan, R. Asmatulu, M. Ceylan, and A. Jabbarnia. Recent progress on conventional and non-conventional electrospinning processes. *Fibers and Polymers*, 14(8):1235–1247, AUG 2013. doi:10.1007/s12221-013-1235-8.
- [5] Giulio Biagi, Tobias Holmgaard, and Esben Skovsen. Near-field electrospinning of dielectric-loaded surface plasmon polariton waveguides. *Optics Express*, 21(4):4355–4360, FEB 25 2013. doi:10.1364/OE.21.004355.
- [6] J. D. Hulstrøm, M. G. Laursen, M. Odgaard, J. O. Pedersen, and L. H. Østergaard. Fabrication and alignment of nanoscale KNbO₃ fibres. AAU Student project, MAY 25 2012.
- [7] Jorge L. Gomez and Onur Tigli. Zinc oxide nanostructures: From growth to application. *Journal of Materials Science*, 48(2):612, NOV 2013. doi:10.1007/s10853-012-6938-5.
- [8] Suehiro Junya, Nobutaka Nakagawa, Shin-ichiro Hidaka, Makoto Ueda, Kiminobu Imasaka, Mitsuhiro Higashihata, Tatsuo Okada, and Masanori Hara. Dielectrophoretic fabrication and characterization of a ZnO and nanowire-based uv and photosensor. *Nanotechnology*, 17(10):2567–2573, APR 2006. doi:10.1088/0957-4484/17/10/021.
- [9] S.J. Pearton, D.P. Norton, K. Ip, Y.W. Heo, and T. Steiner. Recent progress in processing and properties of zno. *Progress in Materials Science*, 50(3):293–340, 2005. doi:10.1016/j.pmatsci.2004.04.001.

- [10] Zhong Lin Wang. Zinc oxide nanostructures: growth, properties and applications. *Journal of Physics: Condensed Matter*, 16(25):R829, 2004. doi:10.1088/0953-8984/16/25/R01.
- [11] Jingbiao Cui. Zinc oxide nanowires. *Materials Characterization*, 64(0):43–52, 2012. doi:http://dx.doi.org/10.1016/j.matchar.2011.11.017.
- [12] Wikipedia. Wurtzite polyhedra Wikipedia, the free encyclopedia, 2004. [Online; accessed 4-August-2014]. URL: http://commons.wikimedia.org/wiki/File:Wurtzite_polyhedra.png#mediaviewer/File:Wurtzite_polyhedra.png.
- [13] Wikipedia. Wurtzite-unit-cell-3d-balls Wikipedia, the free encyclopedia, 2004. [Online; accessed 4-August-2014]. URL: <http://commons.wikimedia.org/wiki/File:Wurtzite-unit-cell-3D-balls.png#mediaviewer/File:Wurtzite-unit-cell-3D-balls.png>.
- [14] W. C. Lin, Y. C. Lin, C. J. Shih, M. Esashi, and A. A. Seshia. Local synthesis and alignment of zinc oxide nanowires in aqueous solution using microheaters. IEEE Publishing, JAN-FEB 2012. doi:10.1109/MEMSYS.2012.6170223.
- [15] Zhong and Lin Wang. Nanostructures of zinc oxide. *Materialstoday*, 7(7):26–33, JUN 2004. doi:10.1016/S1369-7021(04)00286-X.
- [16] Peter A. Smith, Christopher D. Nordquist, Thomas N. Jackson, Theresa S. Mayer, Benjamin R. Martin, Jeremiah Mbindyo, and Thomas E. Mallouk. Electric-field assisted assembly and alignment of metallic nanowires. *Applied Physics Letters*, 77(9):1399, JUL 2000. doi:10.1063/1.1290272.
- [17] Guihua Yu, Xianglong Li, Charles M. Lieber, and Anyuan Cao. Nanomaterial-incorporated blown bubble films for large-area, aligned nanostructures. *J. Mater. Chem.*, 18(7):728, 2008. doi:10.1039/b713697h.
- [18] Franklin Kim, Serena Kwan, Jennifer Akana, and Peidong Yang. Langmuir-blodgett nanorod assembly. *Journal of the American Chemical Society*, 123(18):4360–4361, MAY 2001. doi:10.1021/ja0059138.
- [19] Christian Borschel, Susann Spindler, Damiana Lerosé, Arne Bochmann, Silke H. Christiansen, Sandor Nietzsche, Michael Oertel, and Carsten Rönning. Permanent bending and alignment of ZnO nanowires. *Nanotechnology*, 22(18):1–9, MAR 2011. doi:10.1088/0957-4484/22/18/185307.
- [20] Andrea Camposeo, Israel Greenfeld, Francesco Tantussi, Stefano Pagliara, Maria Moffa, Francesco Fuso, Maria Allegrini, Eyal Zussman, and Dario Pisignano. Local mechanical properties of electrospun fibers correlate to their internal nanostructure. *Nano Letters*, 13(11):5056–5062, NOV 2013. doi:10.1063/1.2975834.

-
- [21] Chieh Chang, Van H. Tran, Junbo Wang, Yiin-Kuen Fuh, and Liwei Lin. Direct-write piezoelectric polymeric nanogenerator with high energy conversion efficiency. *Nano Letters*, 10(2):726–731, FEB 2010. doi:10.1021/nl9040719.
- [22] Chieh Chang, Kevin Limkrailassiri, and Liwei Lin. Continuous near-field electrospinning for large area deposition of orderly nanofiber patterns. *Applied Physics Letters*, 93(12):123111, SEP 22 2008. doi:10.1063/1.2975834.
- [23] Gobind S. Bisht, Giulia Canton, Alireza Mirsepassi, Lawrence Kuinsky, Seajin Oh, Derek Dunn-Rankin, and Marc J. Madou. Controlled continuous patterning of polymeric nanofibers on three-dimensional substrates using low-voltage near-field electrospinning. *Nano Letters*, 11(4):1831–1837, APR 2011. doi:10.1021/nl2006164.
- [24] M. Bashouti, W. Salalha, M. Brumer, E. Zussman, and E. Lifshitz. Alignment of colloidal cds nanowires embedded in polymer nanofibers by electrospinning. *ChemPhysChem*, 7(1):102–106, 2006. doi:10.1002/cphc.200500428.
- [25] M. Rinaldi, F. Ruggieri, L. Lozzi, and S. Santucci. Well-aligned TiO₂ nanofibers grown by near-field-electrospinning. *Journal of Vacuum Science & Technology B*, 27(4):1829–1833, JUL 2009. doi:10.1116/1.3154516.
- [26] Guoping Dong, Yingzhi Chi, Xiudi Xiao, Xiaofeng Liu, Bin Qian, Zhi-jun Ma, E. Wu, Heping Zeng, Danping Chen, and Jianrong Qiu. Fabrication and optical properties of Y₂O₃: Eu³⁺ nanofibers prepared by electrospinning. *Optics Express*, 17(25):22514–22519, DEC 7 2009. doi:10.1149/1.3141425.

List of Lab work

A disc is attached the physical print of the thesis, the content is listed in this appendix.

Top-Down Microscope\	Sol1_1300V1500mum01.jpeg
14-04-06\	Sol1_1300V1500mum02.jpeg
make_plots.m	Sol1_1300V1500mum03.jpeg
makeplot.m	Sol1_1300V1500mum04.jpeg
makeplotdark.m	Sol1_1300V1500mum05.jpeg
runmakeplots.m	<hr/>
Sol1_1300V1000muma01.tif	14-05-22\
Sol1_1300V1000muma02.tif	make_plots.m
Sol1_1300V1000muma03.tif	makeplot.m
Sol1_1300V1000muma04.tif	makeplotdark.m
Sol1_1300V1000muma05.tif	runmakeplots.m
Sol1_1300V1000mumb01.tif	Fab0405_1450V1000mum0101.tif
Sol1_1300V1000mumb02.tif	Fab0405_1450V1000mum0102.tif
Sol1_1300V1000mumb03.tif	Fab0405_1450V1000mum0103.tif
Sol1_1300V1000mumb04.tif	Fab0405_1450V1000mum0104.tif
Sol1_1300V1000mumb05.tif	Fab0405_1450V1000mum0105.tif
Sol1_1300V1500mum01.tif	Fab0405_1450V1000mum0201.tif
Sol1_1300V1500mum02.tif	Fab0405_1450V1000mum0202.tif
Sol1_1300V1500mum03.tif	Fab0405_1450V1000mum0203.tif
Sol1_1300V1500mum04.tif	Fab0405_1450V1000mum0204.tif
Sol1_1300V1500mum05.tif	Fab0405_1450V1000mum0205.tif
Scaled\	Fab0405_1450V1000mum0301.tif
Sol1_1300V1000muma01.jpeg	Fab0405_1450V1000mum0302.tif
Sol1_1300V1000muma02.jpeg	Fab0405_1450V1000mum0303.tif
Sol1_1300V1000muma03.jpeg	Fab0405_1450V1000mum0304.tif
Sol1_1300V1000muma04.jpeg	Fab0405_1450V1000mum0305.tif
Sol1_1300V1000muma05.jpeg	Scaled\
Sol1_1300V1000mumb01.jpeg	Fab0405_1450V1000mum0101.jpeg
Sol1_1300V1000mumb02.jpeg	Fab0405_1450V1000mum0102.jpeg
Sol1_1300V1000mumb03.jpeg	Fab0405_1450V1000mum0103.jpeg
Sol1_1300V1000mumb04.jpeg	Fab0405_1450V1000mum0104.jpeg
Sol1_1300V1000mumb05.jpeg	Fab0405_1450V1000mum0105.jpeg
	Fab0405_1450V1000mum0201.jpeg

A. LIST OF LAB WORK

Fab0405_1450V1000mum0202.jpeg	Fab03-08Zx25.tif
Fab0405_1450V1000mum0203.jpeg	Fab03-08Zx250.tif
Fab0405_1450V1000mum0204.jpeg	Fab03-08Zx2500.tif
Fab0405_1450V1000mum0205.jpeg	Fab03-08Zx25000.tif
Fab0405_1450V1000mum0301.jpeg	Fab03-09aZx2500.tif
Fab0405_1450V1000mum0302.jpeg	Fab03-09Zx25.tif
Fab0405_1450V1000mum0303.jpeg	Fab03-09Zx250.tif
Fab0405_1450V1000mum0304.jpeg	Fab03-09Zx2500.tif
Fab0405_1450V1000mum0305.jpeg	Fab03-09Zx25000.tif
Scanning Electron Microscope	Fab03-10Zx25.tif
2014-03-26	Fab03-10Zx250.tif
#1-01.tif	Fab03-10Zx2500.tif
#1-01A.tif	Fab03-10Zx25000.tif
2014-04-07	Fab03-11Zx25.tif
Fab03-01Zx25.tif	Fab03-11Zx250.tif
Fab03-01Zx250.tif	Fab03-11Zx2500.tif
Fab03-01Zx2500.tif	Fab03-11Zx25000.tif
Fab03-02Zx25.tif	Fab03-12Zx25.tif
Fab03-02Zx250.tif	Fab03-12Zx250.tif
Fab03-02Zx2500.tif	Fab03-12Zx2500.tif
Fab03-02Zx25000.tif	Fab03-12Zx25000.tif
Fab03-03Zx25.tif	Fab03-13Zx25.tif
Fab03-03Zx250.tif	Fab03-13Zx250.tif
Fab03-03Zx2500.tif	Fab03-13Zx2500.tif
Fab03-03Zx25000.tif	Fab03-13Zx25000.tif
Fab03-04Zx25.tif	Fab03-14Zx25.tif
Fab03-04Zx250.tif	Fab03-14Zx250.tif
Fab03-04Zx2500.tif	Fab03-14Zx2500.tif
Fab03-04Zx25000.tif	Fab03-14Zx25000.tif
Fab03-05Zx25.tif	2014-04-11
Fab03-05Zx250.tif	Fab02-01Zx25.tif
Fab03-05Zx2500.tif	Fab02-01Zx250.tif
Fab03-05Zx25000.tif	Fab02-01Zx2500.tif
Fab03-06Zx25.tif	Fab02-02Zx25.tif
Fab03-06Zx250.tif	Fab02-02Zx250.tif
Fab03-06Zx2500.tif	Fab02-02Zx2500.tif
Fab03-06Zx25000.tif	Fab02-03Zx25.tif
Fab03-07Zx25.tif	Fab02-03Zx250.tif
Fab03-07Zx250.tif	Fab02-03Zx2500.tif
Fab03-07Zx2500.tif	Fab02-04Zx25.tif
Fab03-07Zx25000.tif	Fab02-04Zx250.tif
Fab03-08aZx25.tif	Fab02-04Zx2500.tif
Fab03-08aZx250.tif	Fab02-05Zx25.tif
Fab03-08aZx2500.tif	Fab02-05Zx250.tif
Fab03-08aZx25000.tif	Fab02-05Zx2500.tif
	Fab02-09Zx25.tif

Fab03CZx25.tif	Fab03-09Zx2500.tif
Fab03CZx250.tif	Fab03-10Zx25.tif
Fab03CZx2500.tif	Fab03-10Zx250.tif
Fab03S-01Zx25.tif	Fab03-10Zx2500.tif
Fab03S-01Zx250.tif	Fab03-11Zx25.tif
Fab03S-01Zx2500.tif	Fab03-11Zx250.tif
Fab03S-01Zx25000.tif	Fab03-11Zx2500.tif
Fab03S-02Zx25.tif	Fab03-11Zx25000.tif
Fab03S-02Zx250.tif	Fab03-12Zx25.tif
Fab03S-02Zx2500.tif	Fab03-12Zx250.tif
Fab03S-02Zx25000.tif	Fab03-12Zx2500.tif
Fab03S-03Zx25.tif	Fab03-12Zx25000.tif
Fab03S-03Zx250.tif	Fab03-12Zx25000a.tif
Fab03S-03Zx2500.tif	Fab03-13Zx25.tif
Fab03S-03Zx25000.tif	Fab03-13Zx250.tif
2014-04-24\	Fab03-13Zx2500.tif
Fab03-01Zx25.tif	Fab03-13Zx25000.tif
Fab03-01Zx250.tif	Fab03-14Zx25.tif
Fab03-01Zx2500.tif	Fab03-14Zx250.tif
Fab03-01Zx25000.tif	Fab03-14Zx2500.tif
Fab03-02Zx25.tif	2014-05-20\
Fab03-02Zx250.tif	Fab04-01Zx25.tif
Fab03-02Zx2500.tif	Fab04-01Zx250.tif
Fab03-03Zx25.tif	Fab04-01Zx2500.tif
Fab03-03Zx250.tif	Fab04-02Zx25.tif
Fab03-03Zx2500.tif	Fab04-02Zx250.tif
Fab03-03Zx2500a.tif	Fab04-02Zx2500.tif
Fab03-04Zx25.tif	Fab04-03Zx25.tif
Fab03-04Zx250.tif	Fab04-03Zx250.tif
Fab03-04Zx2500.tif	Fab04-03Zx2500.tif
Fab03-05Zx25.tif	Fab04-04Zx25.tif
Fab03-05Zx250.tif	Fab04-04Zx250.tif
Fab03-05Zx2500.tif	Fab04-04Zx2500.tif
Fab03-05Zx25000.tif	Fab04-05Zx25.tif
Fab03-06Zx25.tif	Fab04-05Zx250.tif
Fab03-06Zx250.tif	Fab04-05Zx2500.tif
Fab03-06Zx2500.tif	Fab04-06Zx25.tif
Fab03-07Zx25.tif	Fab04-06Zx250.tif
Fab03-07Zx250.tif	Fab04-06Zx2500.tif
Fab03-07Zx2500.tif	Fab04-07Zx25.tif
Fab03-07Zx25000.tif	Fab04-07Zx250.tif
Fab03-08Zx25.tif	Fab04-07Zx2500.tif
Fab03-08Zx250.tif	Fab04-08Zx25.tif
Fab03-08Zx2500.tif	Fab04-08Zx250.tif
Fab03-09Zx25.tif	Fab04-08Zx2500.tif
Fab03-09Zx250.tif	Fab04-09Zx25.tif

A. LIST OF LAB WORK

Fab04-09Zx250.tif	Fab04-05T-03Zx25.tif
Fab04-09Zx2500.tif	Fab04-05T-03Zx250.tif
Fab05-01Zx25.tif	Fab04-05T-03Zx2500.tif
Fab05-01Zx250.tif	Fab04-05T-04Zx250.tif
Fab05-01Zx2500.tif	Fab04-05T-04Zx2500.tif
Fab05-02Zx25.tif	Fab04U-01Zx25.tif
Fab05-02Zx250.tif	Fab04U-01Zx250.tif
Fab05-02Zx2500.tif	Fab04U-01Zx2500.tif
Fab05-03Zx25.tif	Fab04U-02Zx25.tif
Fab05-03Zx250.tif	Fab04U-02Zx250.tif
Fab05-03Zx2500.tif	Fab04U-02Zx2500.tif
Fab05-04Zx25.tif	Fab04U-03Zx25.tif
Fab05-04Zx250.tif	Fab04U-03Zx250.tif
Fab05-04Zx2500.tif	Fab04U-03Zx2500.tif
Fab05-05Zx25.tif	Fab04U-03Zx2500b.tif
Fab05-05Zx250.tif	Fab04U-04Zx25.tif
Fab05-05Zx2500.tif	Fab04U-04Zx250.tif
Fab05-06Zx25.tif	Fab04U-04Zx2500.tif
Fab05-06Zx250.tif	Fab04U-05Zx25.tif
Fab05-06Zx2500.tif	Fab04U-05Zx250.tif
Fab05-07Zx25.tif	Fab04U-05Zx2500.tif
Fab05-07Zx250.tif	Fab04U-06Zx25.tif
Fab05-07Zx2500.tif	Fab04U-06Zx250.tif
Fab05-08Zx25.tif	Fab04U-06Zx2500.tif
Fab05-08Zx250.tif	Fab04U-06Zx2500b.tif
Fab05-08Zx2500.tif	Fab04U-07Zx25.tif
Fab05-09Zx25.tif	Fab04U-07Zx250.tif
Fab05-09Zx250.tif	Fab04U-07Zx2500.tif
Fab05-09Zx2500.tif	Fab04U-07Zx2500b.tif
Fab05-10Zx25.tif	Fab04U-08Zx25.tif
Fab05-10Zx250.tif	Fab04U-08Zx250.tif
Fab05-10Zx2500.tif	Fab04U-08Zx2500.tif
Fab05-11Zx25.tif	Fab04U-09Zx25.tif
Fab05-11Zx250.tif	Fab04U-09Zx250.tif
Fab05-11Zx2500.tif	Fab04U-09Zx2500.tif
Fab05-12Zx25.tif	Fab04U-09Zx25000.tif
Fab05-12Zx250.tif	Fab04U-10Zx25.tif
Fab05-12Zx2500.tif	Fab04U-10Zx250.tif
2014-05-21 \	Fab04U-10Zx2500.tif
Fab04-05T-01Zx25.tif	Fab05U-01Zx25.tif
Fab04-05T-01Zx250.tif	Fab05U-01Zx250.tif
Fab04-05T-01Zx2500.tif	Fab05U-01Zx2500.tif
Fab04-05T-02Zx25.tif	Fab05U-02Zx25.tif
Fab04-05T-02Zx250.tif	Fab05U-02Zx250.tif
Fab04-05T-02Zx2500.tif	Fab05U-02Zx2500.tif

Fab05U-03Zx25.tif
Fab05U-03Zx250.tif
Fab05U-03Zx2500.tif
Fab05U-04Zx25.tif
Fab05U-04Zx250.tif
Fab05U-04Zx2500.tif
Fab05U-05Zx25.tif
Fab05U-05Zx250.tif
Fab05U-05Zx2500.tif
Fab05U-06Zx25.tif
Fab05U-06Zx250.tif
Fab05U-06Zx2500.tif
Fab05U-07Zx25.tif
Fab05U-07Zx250.tif
Fab05U-07Zx2500.tif
Fab05U-08Zx25.tif
Fab05U-08Zx250.tif
Fab05U-08Zx2500.tif
Fab05U-09Zx25.tif
Fab05U-09Zx250.tif
Fab05U-09Zx2500.tif
2014-05-22
Fab0405NFES-01Zx25.tif
Fab0405NFES-01Zx250.tif
Fab0405NFES-01Zx2500.tif
Fab0405NFES-01Zx25000.tif
Fab0405NFES-02Zx25.tif
Fab0405NFES-02Zx250.tif
Fab0405NFES-02Zx2500.tif
Fab0405NFES-03Zx25.tif
Fab0405NFES-03Zx250.tif
Fab0405NFES-03Zx2500.tif
Fab0405NFES-03Zx25000.tif
Fab0405NFES-04Zx25.tif
Fab0405NFES-04Zx250.tif
Fab0405NFES-04Zx2500.tif
Fab0405NFES-05Zx25.tif
Fab0405NFES-05Zx250.tif
Fab0405NFES-05Zx2500.tif
Fab0405NFESB-01Zx25.tif
Fab0405NFESB-01Zx250.tif
Fab0405NFESB-01Zx2500.tif
Fab0405NFESB-02Zx25.tif
Fab0405NFESB-02Zx250.tif
Fab0405NFESB-03Zx25.tif

Fab0405NFESB-03Zx250.tif
Fab0405NFESB-03Zx2500.tif
Fabrication ZnO nanowires.xlsx
MasterThesis.pdf